

Highly heterogeneous genomic landscape of uterine leiomyomas by whole exome sequencing and genome-wide arrays

Svetlana A. Yatsenko, M.D.,^{a,b,c} Priya Mittal, Ph.D.,^{c,d,e} Michelle A. Wood-Trageser, Ph.D.,^f Mirka W. Jones, M.D.,^b Urvashi Surti, Ph.D.,^{a,b,c,d} Robert P. Edwards, M.D.,^{a,d} Anil K. Sood, M.D.,^g and Aleksandar Rajkovic, M.D., Ph.D.^{a,b,c,d}

^a Department of Obstetrics, Gynecology, and Reproductive Sciences, University of Pittsburgh, Pittsburgh, Pennsylvania;

^b Department of Pathology, Magee-Women's Hospital of University of Pittsburgh Medical Center, Pittsburgh, Pennsylvania; ^c Department of Human Genetics, Graduate School of Public Health, University of Pittsburgh, Pittsburgh, Pennsylvania; ^d Magee-Women's Research Institute, Pittsburgh, Pennsylvania; ^e Department of Oncology, St. Jude Children's Research Hospital, Memphis, Tennessee; ^f Department of Pathology, Starzl Transplantation Institute, University of Pittsburgh, Pittsburgh, Pennsylvania; and ^g Department of Gynecologic Oncology and Cancer Biology, University of Texas MD Anderson Cancer Center, Houston, Texas

Objective: To determine the genomic signatures of human uterine leiomyomas and prevalence of *MED12* mutations in human uterine leiomyosarcomas.

Design: Retrospective cohort study.

Setting: Not applicable.

Patient(s): This study included a set of 16 fresh frozen leiomyoma and corresponding unaffected myometrium specimens as well as 153 leiomyosarcomas collected from women diagnosed with uterine leiomyomas or leiomyosarcomas who underwent clinically indicated abdominal hysterectomy.

Intervention(s): None.

Main Outcome Measure(s): Whole exome sequencing and high-resolution X-chromosome and whole genome single nucleotide polymorphism microarray analyses were performed on leiomyoma samples negative for the known *MED12* mutations and compared with their corresponding myometrium. Leiomyosarcoma specimens were examined for exon 2 *MED12* mutations to evaluate the frequency of *MED12* mutated leiomyosarcomas.

Result(s): Our results indicate remarkable genomic heterogeneity of leiomyoma lesions. *MED12*-negative leiomyomas contain copy number alterations involving the Mediator complex subunits such as *MED8*, *MED18*, *CDK8*, and long intergenic nonprotein coding RNA340 (CASC15), which may affect the Mediator architecture and/or its transcriptional activity. We also identified mutations in a number of genes that were implicated in leiomyomagenesis such as *COL4A6*, *DCN*, and *AHR*, as well as novel genes: *NRG1*, *ADAM18*, *HUWE1*, *FBXW4*, *FBXL13*, and *CAPRIN1*.

Conclusion(s): Mutations in genes implicated in cell-to-cell interactions and remodeling of the extracellular matrix and genomic aberrations involving genes coding for the Mediator complex subunits were identified in uterine leiomyomas. Additionally, we discovered that ~4.6% of leiomyosarcomas harbored *MED12* exon 2 mutations, but the relevance of this association with molecular pathogenesis of leiomyosarcoma remains unknown. (Fertil Steril® 2017;107:457–66. ©2016 by American Society for Reproductive Medicine.)

Key Words: Uterine leiomyoma, uterine leiomyosarcoma, *MED12* mutation negative, whole exome sequencing, whole genome copy number analysis

Discuss: You can discuss this article with its authors and with other ASRM members at <https://www.fertsterdialog.com/users/16110-fertility-and-sterility/posts/12942-22775>

Received July 15, 2016; revised and accepted October 26, 2016; published online November 23, 2016.

S.A.Y. has nothing to disclose. P.M. has nothing to disclose. M.A.W.-T. has nothing to disclose. M.W.J. has nothing to disclose. U.S. has nothing to disclose.

R.P.E. has nothing to disclose. A.K.S. has nothing to disclose. A.R. has nothing to disclose.

This study was funded by Magee Women's Research Institute and Foundation.

Reprint requests: Aleksandar Rajkovic, M.D., Ph.D., Professor, Marcus Allen Hogge Chair in Reproductive Sciences, Department of Obstetrics and Gynecology and Reproductive Sciences, University of Pittsburgh, Magee Women's Research Institute, 204 Craft Avenue, Pittsburgh, Pennsylvania 15213 (E-mail: rajkovic@upmc.edu).

Uterine smooth muscle tumors are the most common solid uterine neoplasm and are found in more than 50% of women (1, 2). Usually these tumors are benign, known as uterine leiomyomas (ULs) or fibroids. ULs comprise cells that resemble the uterine myometrium, however, their origin is still under investigation (3, 4). ULs requiring treatment cause significant morbidity and are associated with symptoms such as dysmenorrhea, menorrhagia, infertility, miscarriage, ascites, anemia, and polycythemia. Nearly half of all ULs show normal karyotype, while the other half harbors various cytogenetic aberrations (5). Whole exome approaches have identified heterozygous somatic mutations confined to exon 2 of the Mediator complex subunit 12 (*MED12*, OMIM *300188) in about 70% of ULs (6, 7). *MED12* protein is a part of the evolutionarily conserved Mediator complex and is involved in transcriptional regulation of the RNA polymerase II initiation complex. Our previous studies showed that the *MED12* c.131G>A mutation induces ULs via a gain-of-function mechanism and is a precursor to genomic instability, often observed in ULs (7–9). Among *MED12* mutation-negative ULs, somatic cytogenetic alterations involving the *HMGA2* gene (OMIM 600698; at 12q14.3), or rare biallelic inactivation of the *FH* gene (OMIM 136850; at 1q43), have also been implicated in tumor initiation processes in fewer than 70%–10% of cases. The remaining 20%–23% of ULs are of unknown etiology.

In rare cases, uterine smooth muscle tumors are malignant, with an incidence of less than 0.001%. Uterine LMs (ULMs) are clinically aggressive, highly recurrent tumors with poor prognosis and survival. The etiology and genetic alterations associated with ULMs are poorly understood. Despite notable phenotypic differences between the malignant and benign tumors, the presence of *MED12* mutations in some ULMs samples raises a question of whether a subset of ULMs may arise from preexisting ULs (10).

The aims of this study were to investigate genomic integrity at the *MED12* locus (Xq13.1), explore a possibility of gain-of-function-activating mutations through duplication or triplication of the *MED12* gene or copy number alterations within the gene vicinity, and discover novel driver oncogenes in *MED12* mutation-negative ULs. In addition, we screened the largest cohort of ULMs for *MED12* exon 2 variants.

MATERIALS AND METHODS

Specimens

This study was approved by the Institutional Review Board of the University of Pittsburgh (IRB no. PRO12010246). All ULM samples were derived from specimens that were originally obtained only for purposes of clinical treatment or pathological evaluation, and specimens did not contain any personal identifiers or linkage codes. Samples were collected from women who were diagnosed with ULs or ULMs and who underwent medically indicated abdominal hysterectomy.

A total of 148 UL specimens collected from 1988–1991 for previous study were obtained from the Magee-Women's Hospital of University of Pittsburgh Medical Center. Part of each sample was fresh frozen, and a portion was set up in culture for cytogenetic analysis (11). Conventional karyotype

analysis was performed according to the standard G-banding techniques. A minimum of 20 metaphase cells were evaluated after 5–10 days of culturing at the 400–450 band resolution.

A total of 153 formalin-fixed paraffin-embedded (FFPE) or frozen LMs were obtained from Magee-Women's Hospital of University of Pittsburgh Medical Center and MD Anderson Cancer Center. The histology was reviewed by a board-certified gynecologic pathologists.

Nucleic Acid Extraction and Preparation

Genomic DNAs from all ULs and corresponding myometrial samples were extracted from 100 mg of freshly frozen tissue using the Gentra Puregene Blood Kit (Qiagen), according to the manufacturer's protocol. DNA quality was verified through Nanodrop and Qubit analysis, and integrity of gDNA was examined by running 250 ng on a 0.8% agarose gel. Genomic DNAs from LMs were either extracted from frozen samples as described above or from FFPE sections according to the method described elsewhere (12) using the DNeasy Blood and Tissue Kit (Qiagen).

MED12 Exon 2 Mutation Screening

In total, 148 UL samples (7) and 153 ULMs were screened for variants in exon 2 of *MED12* via Sanger sequencing. Oligonucleotide primers (forward primer 5'-TAGTGAC-CATGGGAGTGAGG-3' and reverse primer 5'-GAAGG-CAAATCAGC CACTAG-3') were designed to amplify exon 2 of *MED12* using Primer3 (<http://frodo.wi.mit.edu/primer3/>) software. Genomic DNAs were amplified with *ampli*-*sure* PCR Master Mix (GeneDEPOT) under the following conditions: 94°C for 3 minutes; 35 cycles of 94°C for 30 seconds, 60°C for 15 seconds, 72°C for 30 seconds; and 72°C for 2 minutes. DNA sequences were evaluated using Sequencher 5.1 software (Gene Codes Corp.). Overall, 100/148 ULs were positive for *MED12* mutations and reported elsewhere (7), while 48 ULs were negative for the *MED12* gene alterations. UL samples lacking *MED12* mutations were used in this study.

X-chromosome Copy Number Analysis

High-resolution X-chromosome copy number profiling was performed using the 180K comparative genomic hybridization (CGH) microarray, according to manufacturers' instructions (Agilent Technologies). To detect X-chromosome copy number variations (CNVs) with the resolution of 0.3–1 kb we constructed a custom CGH microarray with probes covering the entire X-chromosome. The high-resolution X-chromosome array (X-HR) contains 180,000 unique 60-mer oligonucleotide probes with a spacing of 5–8 interrogating oligonucleotide probes per 1 kb within the focused gene- and exon-based regions, with an average genomic spacing of one probe per 1 kb for the X-chromosome and three to four probes per 1 Mb for the other regions of the genome. The data analysis was performed as described elsewhere (13). Aberrant regions were displayed using the Cytogenomics 2.5 (Agilent) software. Ten fresh frozen UL specimens (L4, L5, L33, L34, L42, L48, L49, L56, L59, L68) were studied by X-HR (Supplemental Table 1).

Whole Genome Copy Number Analysis

Whole genome copy number profiling was performed using the Illumina HumanOmniExpressExome-8v1 (Illumina) Beadchip (L33, L34, L42, L48, L49, L59, L63, L60, L68, and L69) or the 180K CGH+ single nucleotide polymorphism (SNP) platform (ISCA design, Agilent; L56, L58, L64, and L70; *Supplemental Table 1*), with the average genomic resolution of 100 kb and 6–20 kb for gene-coding regions. Array CGH experiments were performed using a normal female reference DNA (Coriell NA12878). Standard cluster file was used to calculate both intensity \log_2 ratio and B-allele frequency. Aberrant regions were identified by the cnv/partition plug-in algorithm for CNV detection (KaryoStudio, Illumina) or by aberration algorithm ADM-2 with a moving average of five consecutive probes per region (Cytogenomics 2.5, Agilent) software. DNA CNVs were eliminated from further investigation if these CNVs were in regions containing no known genes or regulatory sequences or were present in the UL or myometrium samples at the same frequency as in peripheral blood samples from a general population based on the Database of Genomic Variants (<http://projects.tcag.ca>).

Whole Exome Sequencing (WES)

Genomic DNA from 13 pairs of samples (13 leiomyomas and 13 corresponding myometrial samples: L4/M4, L5/M5, L34/M34, L42/M42, L48/M48, L49/M49, L58/M58, L59/M59, L60/M60, L64/M64, L68/M68, L69/M69, and L70/M70; *Supplemental Table 1*) were subjected to in-solution exome enrichment via the SureSelect Human All Exon Kit v4+UTRs (Agilent). After exome capture, the samples were submitted for 2×100 bp paired end high-throughput sequencing on the HiSeq 2000 (Illumina). The average coverage of target intervals of these samples is from $60\times$ to $320\times$. See more details in the *Supplemental Data*. Raw data were deposited into the Sequencing Reads Archive (<https://submit.ncbi.nlm.nih.gov/subs/sra/>) accession number PRJNA319022.

RESULTS

Forty-eight UL samples previously determined to be negative for the known *MED12* mutations in exon 2 were further evaluated for the presence of other genomic alterations. Culturing of four tumor specimens showed no growth precluding karyotype analysis. Eighteen of 44 (41%) samples had abnormal findings by karyotype (*Supplemental Table 2*), while the remaining 26 UL specimens showed an apparently normal 46,XX chromosome complement. A set of 16 pairs (UL with corresponding myometrium) negative for both *MED12* mutations and karyotypic abnormalities was subjected to further testing including whole-genome CNV analysis (14 samples), X-chromosome high-resolution CNV profiling (10 samples), and WES (13 samples; *Supplemental Table 1*). Overall, 13 UL samples had significant findings, and three ULs were negative for alterations.

X-chromosome CNVs in *MED12*-negative Leiomyomas

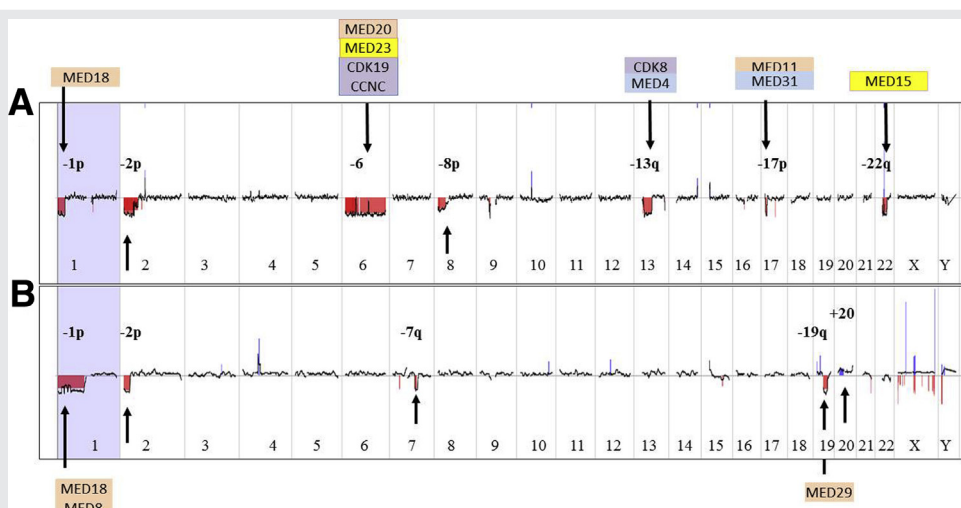
We used X-HR microarray to examine UL samples negative for *MED12* mutations and cytogenetically visible chromo-

somal abnormalities for the presence of genomic imbalances involving the Xq13.1 (*MED12* locus), other genes on the X-chromosome, and autosomal genes implicated in the development and function of a female genitourinary tract. *MED12* is located on the X-chromosome, and X-HR provides unprecedented resolution at a few hundred base pairs to detect CNVs that other microarray designs may not be able to detect. A total of 68 single copy number changes (47 gains and 21 losses) were identified in tumor samples. Out of these, seven CNVs from four cases were novel alterations (*Supplemental Table 3*). In these four samples (L34, L48, L49, L68) we identified cryptic X-chromosome CNVs, ranging from 322 bp to 144.6 kb. Interestingly, a gain encompassing exon 21 of the *COL4A6* gene (OMIM 303631) was found in L34, which is predicted to result in a frameshift mutation. In patient L48, we detected a deletion involving exons 6–8 of the *TFE3* gene (OMIM 314310), which is implicated in progression of various tumors including renal carcinomas. A gain of ~ 73.5 kb region involving the entire *VBP1* gene (Von Hippel-Lindau binding protein 1, OMIM 300133) was detected in L49. Remarkably, Von Hippel-Lindau syndrome is a familial cancer condition with predisposition to malignant and benign neoplasms such as retinal hemangioblastoma and renal cell carcinoma. Lastly, in patient L68 we detected a 144.6-kb gain encompassing the *EDA2R* gene (OMIM 300276), which is involved in various tumor signaling pathways. Overall, microarrays did not detect any submicroscopic deletions or duplications encompassing the *MED12* gene or involving the 1-Mb sequences upstream and downstream of the gene, excluding copy number alterations within putative distant-acting regulatory elements.

Autosomal CNVs in *MED12*-negative Leiomyomas

Copy number profiles were obtained on 14 UL samples. In nine specimens (64.3%) we detected somatic copy number alterations, ranging from 0.163 to 197.8 Mb, involving autosomes (L33, L48, L56, L58, L60, L63, L64, L69, and L70; *Supplemental Table 4*). Despite the normal G-banded chromosome findings obtained on cultured metaphase cells, gross chromosomal aberrations were present in 8/14 (57%) samples, and one sample L48 had a submicroscopic 6p deletion. Two UL samples (L33 and L69) harbored a pathologically relevant loss on chromosome 1q, encompassing the *FH* gene (fumarate hydratase, OMIM 136850). Tumor sample L64 was found to carry a 257-kb deletion at the 3' end of the *HMGA2* gene, suggestive of *HMGA2* rearrangement. Remarkably, L48 was found to contain a 213-kb deletion comprising the long noncoding RNA (CASC15, cancer susceptibility candidate 15), which has been implicated in pre- and post-transcriptional gene regulation and cancer progression. Four samples (L56, L58, L64, and L69) had multiple large chromosomal alterations. Interestingly, multiple components of the Mediator complex such as *MED8*, *MED18*, and *MED29* were located within the deleted regions in these tumor samples (*Supplemental Table 4*). Multiple genomic alterations were present in L58, encompassing at least 10 subunits of the Mediator complex (Fig. 1). Thus, multiple CNVs were identified in

FIGURE 1



Whole genome array CGH (aCGH) in UL samples L56 and L58. **(A)** Whole genome profile in L58. Black scatter plot shows the average log₂ ratio for the aCGH probes that are arranged from the short to the long arm of each chromosome. Chromosomes are listed at the bottom. Copy number losses involving chromosomes 1p, 2p, 6, 8p, 13q, 17p, and 22q (red shaded areas) encompass multiple subunits of the Mediator complex. Components of Mediator corresponding to the head, middle, tail, or the dissociable CDK8 kinase module (CKM) are depicted by pink, blue, yellow, and gray color, respectively. **(B)** Whole genome profile demonstrates gross chromosomal alterations (black arrows) in L56 with normal karyotype.

Yatsenko. Genomic landscape of uterine leiomyomas. *Fertil Steril* 2016.

MED12-negative tumors, which were previously undetected using classical G-banding karyotyping.

WES of *MED12*-negative ULs

Thirteen pairs of ULs lacking *MED12* exon 2 mutations with apparently normal karyotype and their corresponding myometrium (L4/M4, L5/M5, L34/M34, L42/M42, L48/M48, L49/M49, L58/M58, L59/M59, L60/M60, L64/M64, L68/M68, L69/M69, and L70/M70) were evaluated by WES to investigate for novel recurrent variants. Variants derived from ULs were compared with matched myometrium, and at each position was scored as homozygous, heterozygous, or null for a particular variant. Modeling after *Med12* variants, which are not present in the germline databases, we assumed that de novo variants in ULs that cause tumor growth will not be present with significant frequency in the germline databases. We identified 16 unique variants in 16 genes across six UL samples (Table 1) that satisfied the criteria of a de novo variant in UL, absent or with very low frequency in the germline variant databases (less than 0.1%). Seven out of 13 pairs of ULs did not show significant variants in comparison with a matched myometrium. Twelve of these changes were de novo heterozygous variants found only in leiomyomas that were absent in the matching myometrium. The remaining four variants were heterozygous in the myometrium, while matching leiomyomas were homozygous for the variant. There were no recurring variants in the same gene among the 13 samples that we sequenced.

Genomic Landscape in ULs

To gain insight into the UL pathogenesis and to identify novel driver genes, we examined genomic alterations that are pre-

sent among *MED12*-negative ULs. Chromosomal rearrangements detected by karyotype in 18 cases (Supplemental Table 2) and genomic aberrations revealed by microarray and WES analyses in 13 karyotypically normal UL samples are summarized in Figure 2. The most common and consistent alterations in *MED12*-negative ULs appear to be deletions involving 1q31-q44, 1p34-p36, 2p23-p25, and 22q chromosomal regions, which were detected in 10/31 (32.3%), 7/31 (22.6%), 5/31 (16.1%), and 5/31 (16.1%) samples, respectively. Notably, heterozygous 1q43 deletions encompassing the *FH* gene were detected in eight samples (six studied by karyotype and two by microarray), however, our WES analysis did not identify any mutations that would indicate biallelic *FH* involvement in the tumor. In addition, we observed a clustering of the breakpoints around 12q14 region (Fig. 2), indicating a possibility for the *HMGA2* gene rearrangement in a subset of the cases.

In contrast, genomic alterations in *MED12*-positive ULs (Fig. 3) are very distinct from those observed in *MED12*-negative tumors. Chromosomal rearrangements were detected by karyotype analysis in 31 samples out of 90 (34%) previously reported *MED12*-positive ULs (7), with the vast majority of alterations residing within the 7q21-q31 region discovered in 18/31 (58%) cases. Also, genomic alterations in *MED12*-positive ULs do not appear to affect regions coding for other Mediator complex subunits as seen in *MED12*-negative specimens (Fig. 3).

Prevalence of *MED12* Mutations among ULMs from North American Women

To investigate the molecular basis of ULMs and further elucidate the etiology of these malignant tumors with respect to

TABLE 1List of somatic variants present in *MED12* mutation negative leiomyomas detected by WES.

Sample	Variant	Chromosome band	Gene	Gene function	Variant-type	Nucleotide-change	AA change
L48	SNV	3p21.31	<i>ARIH2OS</i>	Unknown	Missense	exon1:c.C410G	p.Ser137Cys
L49	SNV(hmz)	17q25.3	<i>RAB40B</i>	Regulating secretory vesicles	Missense	exon6:c.C788G	p.Pro263Arg
L49	SNV	8p13.2	<i>PREX2</i>	Unknown	Stop	exon10:c.C1170A	p.Cys 390*
L58	SNV(hmz)	11q12.3	<i>SLC22A10</i>	Transmembrane transporter activity	Missense	exon9:c.C1421T	p.Thr474Met
L58	Insertion	7q22.1	<i>FBXL13</i>	Ubiquitin-protein ligase	Frameshift	exon4:c.211_212insAA	p.Val71Lysfs*2
L58	SNV	8p11.22	<i>ADAM18</i>	Cell-cell and cell-matrix interactions	Missense	exon4:c.A230G	p.Glu77Gly
L59	SNV(hmz)	13q12.3	<i>USPL1</i>	SUMO-specific isopeptidase involved in protein desumoylation	Missense	exon9:c.A3163T	p.Ser1055Cys
L59	SNV(hmz)	11q12.1	<i>TNKS1BP1</i>	Enzyme binding	Missense	exon6:c.A3290G	p.Gln1097Arg
L59	SNV	7p21.1	<i>AHR</i>	Transcription factor, cell-cycle regulation	Missense	exon10:c.G1891A	p.V631Ile
L59	SNV	11p13	<i>CAPRIN1</i>	Cell cycle associated protein	stop	exon3:c.C274T	p.Gln92*
L59	SNV	10q24.32	<i>FBXW4</i>	Ubiquitin mediated degradation	Missense	exon1:c.C11A	p.Ala4Glu
L59	SNV	Xp11.1	<i>HUWE1</i>	Ubiquitin-protein ligase	Stop	exon30:c.C3295T	p.Arg1099*
L59	SNV	6q27	<i>MLLT4</i>	Cell junction organization	Stop	exon4:c.C532T	p.Arg178*
L59	SNV	8p12	<i>NRG1</i>	Cell-cell signaling	Missense	exon3:c.A806G	p.Asn269Ser
L60	Deletion	17q21.2	<i>KAT2A</i>	Histone acetyltransferase	Frameshift	exon10:c.1618_1619del	p.Arg540Profs*12
L64	Deletion	12q21.3	<i>DCN</i>	Tumor suppression	Frameshift	exon2:c.226_233del	p.Pro76Serfs*4

Note: hmz = homozygous change (heterozygous in myometrium, homozygous in leiomyoma); SNV = single nucleotide variant.

Yatsenko. Genomic landscape of uterine leiomyomas. *Fertil Steril* 2016.

their benign counterparts, ULs, we examined exon 2 of *MED12* via targeted DNA sequencing. In our subset of 153 ULMs, we observed heterozygous single nucleotide changes in seven samples (7/153; 4.6%). All ULM histology was confirmed by a board-certified gynecologic pathologist, and tumor tissue used for sequencing was estimated to contain at least 80% of tumor cells. A representative histology and mutation analysis is shown in *Supplemental Figure 1*. All variants occurred at nucleotide positions 130 and 131 in codon 44 and caused the following amino acid changes: p.Gly44Ser (2/153; 1.3%), p.Gly44Ala (2/153; 1.3%), p.Gly44Arg (1/153; 0.7%), p.Gly44Cys (1/153; 0.7%), and p.Gly44Asp (1/153; 0.7%).

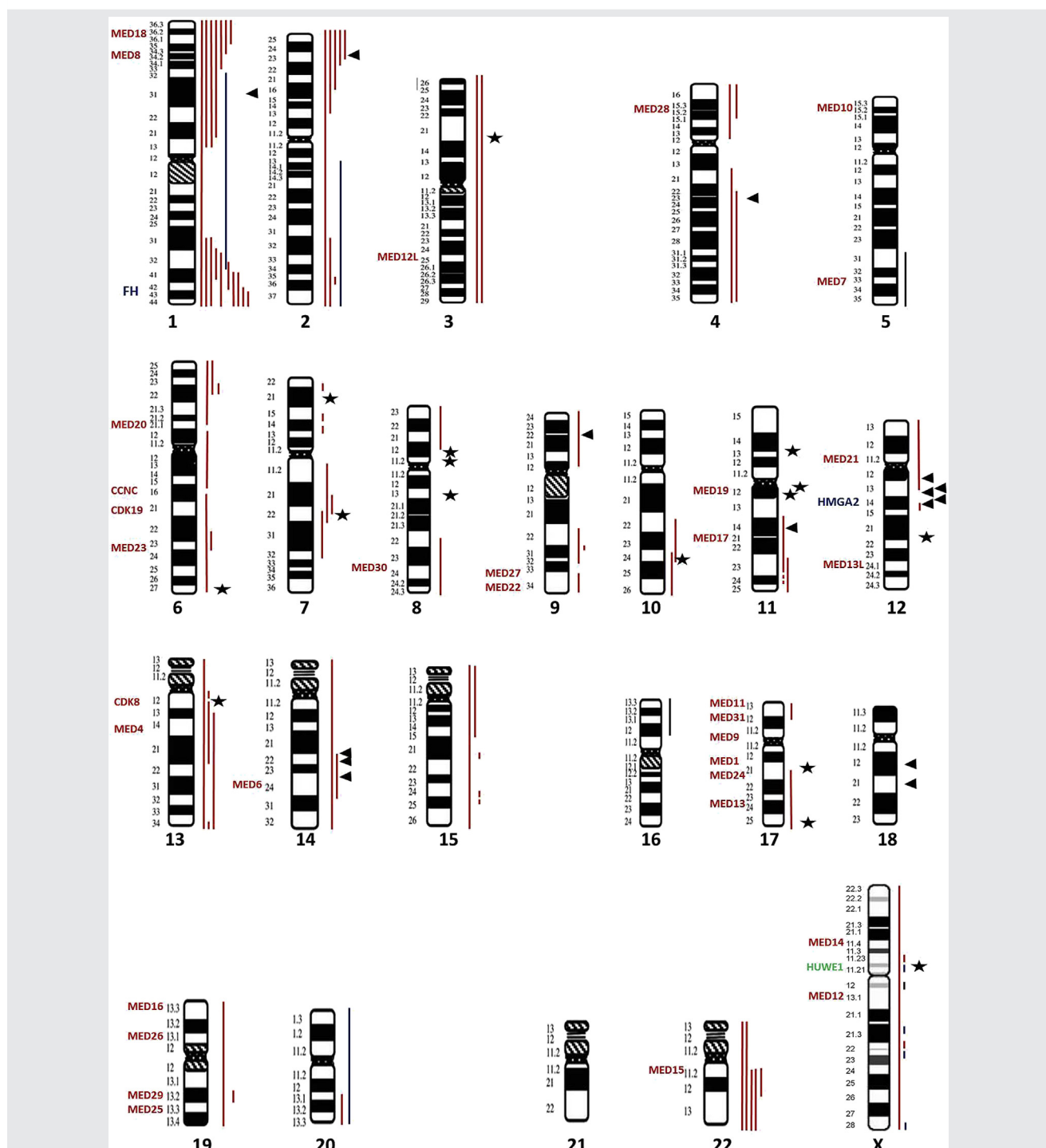
DISCUSSION

Previously, a large subset of ULs (70%) has been associated with heterozygous *MED12* exon 2 and exon 1 mutations among multiple racial and ethnic groups (6,7,14–17). We generated an animal model of *MED12* exon 2 variants and have shown that the *Med12* exon 2 variants induce ULs (9). However, other drivers of leiomyomagenesis are likely to exist, including *HMGA2* aberrant expression (18, 19).

In an attempt to discover other novel driver mutations in *MED12* mutation-negative and karyotypically normal ULs,

we conducted a comprehensive genomic evaluation for copy number alterations and WES on pairs of UL and matched myometrium samples. Similar to the previous studies (7, 20), WES on *MED12*-negative ULs did not identify recurrent mutations in a specific gene or mutations in previously known UL driver genes such as *FH*, *COL4A6*, or *HMGA2*, nor in *MED12* exon 1, that could explain the initiation events in ULs. However, we detected two samples with cryptic heterozygous copy number alterations involving the *COL4A6* and *HMGA2* gene regions. Whole exome variants identified in *MED12*-negative ULs but absent in matched myometrium were not present in the germline variant databases, as would be expected for somatic variants that are likely to be lethal in the germline. None of the variants were present in the Cancer genome data sets available through cBioPortal (<http://www.cbioperl.org/news.jsp>) or the COSMIC database (<http://cancer.sanger.ac.uk/cosmic>). Seven of the 13 *MED12*-negative ULs showed no difference from the matched myometrium. Six of the 13 *MED12*-negative ULs showed variants distinct from the matched myometrium (Table 1), with sample L59 having variants in eight genes, L58 having variants in three genes, L49 having variants in two genes, and L48, L60, and L64 each having a variant in one gene. A total of 16 variants were detected, of which 12 represented wild-type (myometrium) to

FIGURE 2



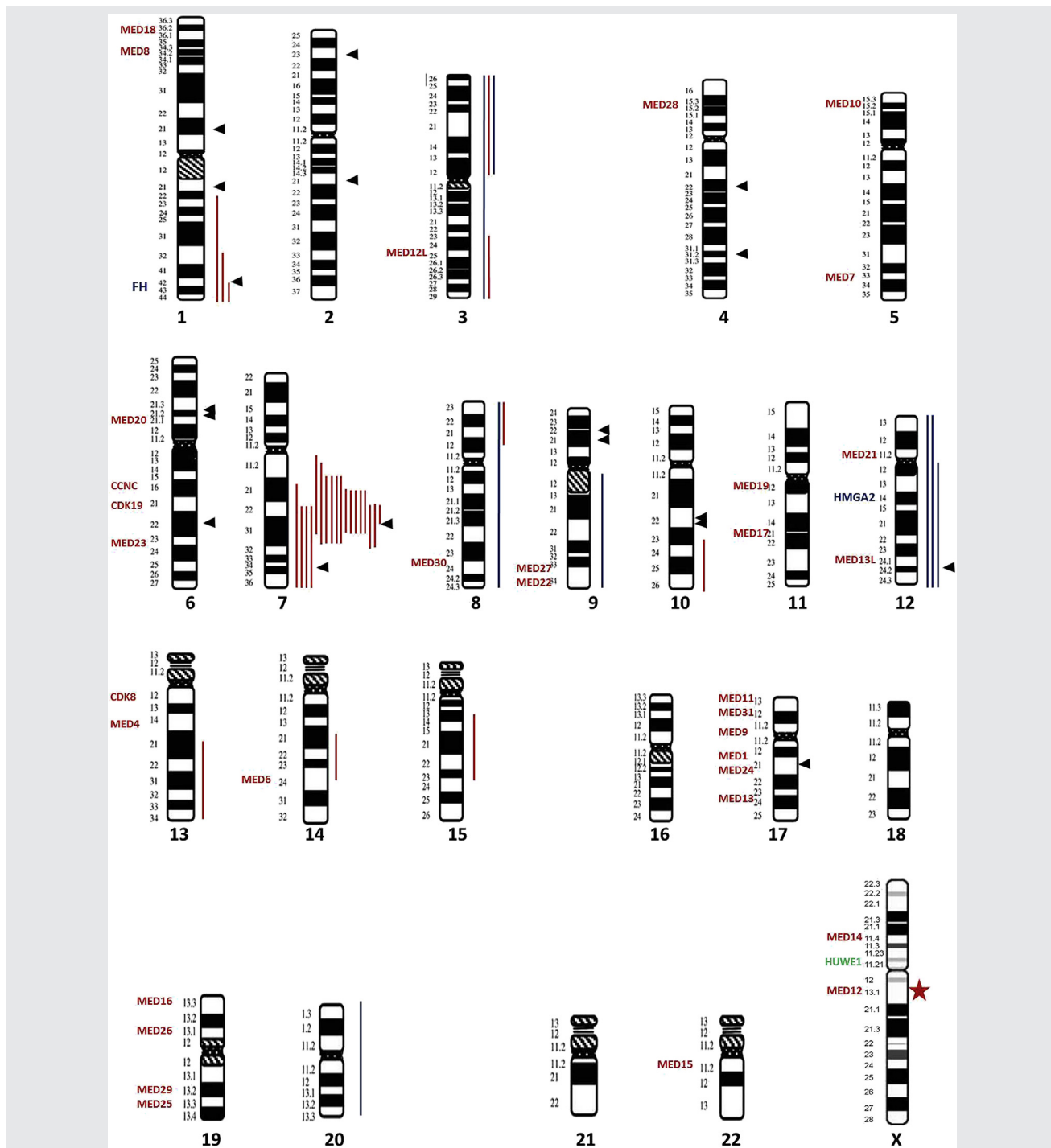
Landscape of genomic aberrations detected by karyotype, microarray, and WES analyses in 31 cases negative for *MED12* exon 2 mutations. Genes coding for subunits of the Mediator complex (in red) and other genes (*FH* and *HMGA2* in blue), implicated in UL pathogenesis, are shown through the human genome. Red lines to the right of the idiograms indicate loss of chromosomal material, and black lines indicate gain of chromosomal material. Black triangles represent translocation breakpoints in tumor samples. Stars indicate gene mutations.

Yatsenko. Genomic landscape of uterine leiomyomas. *Fertil Steril* 2016.

heterozygous change (leiomyoma) and four represented heterozygous (myometrium) to homozygous (leiomyoma) change. Although neither common variants nor common genes were present across multiple ULs, a subset of discovered

variants was in genes previously studied in association with ULs or cancer. L64 has a heterozygous frameshift mutation in tumor suppressor gene *decorin*, *DCN*, which was previously associated with keloid scar and colon cancer formation [21],

FIGURE 3



Genomic alterations in *MED12*-positive ULs revealed by karyotype in 31 cases. Red star at Xq13.1 indicates *MED12* mutation.

Yatsenko. Genomic landscape of uterine leiomyomas. *Fertil Steril* 2016.

22). Moreover, previous reports have found altered decorin and remodeled extracellular matrix (ECM) in ULs (23, 24). L59 contained multiple variants including heterozygous variant in the *AHR* (aryl hydrocarbon receptor) gene, a transcription factor involved in cell cycle regulation. Previous reports have indicated dysregulation of *AHR*

expression in ULs (25, 26). The same sample also contained a heterozygous variant in *CAPRIN1*, a cell cycle-associated protein implicated in tumor proliferation (27–29), as well as heterozygous stop mutation in the *HUWE1* gene, which functions as an E3 ubiquitin ligase and has been implicated in myogenesis (30), ECM remodeling, and tumor formation

(31, 32). Another heterozygous variant was detected in ubiquitin-protein ligase gene, *FBXL13*, in L58. Ubiquitin ligases play an important role in the degradation of a wide range of substrates, which are implicated in cell cycle regulation, signal transduction, cell-to-cell junction, and tissue homeostasis, as well as DNA replication, transcriptional regulation, response to DNA damage, and overall genomic integrity. In our cohort, multiple UL samples harbored variants in genes affecting ECM remodeling including *ADAM18* (L58), *MLLT4* (L59), and signal transduction *NRG1* (L59). *MLLT4*, a multidomain protein involved in the organization of cell-cell junctions and signaling has not been directly linked to ULs, however, *MLLT4* has been implicated in oncogenesis and metastasis (33). None of the genes identified by WES in *MED12*-negative ULs are known to encode proteins that induce leiomyomagenesis or interact with FH or *MED12* proteins.

We asked whether copy number changes involving *MED12* were present in *MED12* mutation-negative ULs. We did not observe any cryptic alterations within the *MED12* gene or X-chromosome alterations in the *MED12* regulatory sequences in the ULs lacking *MED12* point mutations. Using whole genome microarray, we observed some typical UL cytogenetic alterations, such as deletions of 1p, 1q, and 2p, which were not detected by G-banding techniques. Interestingly, *HUWE1* was the only gene shared between the array (L34) and the exome sequencing (L59) results from two independent UL samples. *HUWE1*, a tumor suppressor, has been previously implicated in the progression of various tumors (34) and is involved in ubiquination of p53 (35) as well as Cds6, Myc, and Mycn (36–38). We also detected alteration at the *COL4A6* locus (L34; *Supplemental Table 3*). *COL4A6* is important for normal smooth muscle differentiation, and alterations at this locus have previously been associated with ULs (8). Overall, our findings indicate that independent pathways and genomic alterations may contribute to UL pathogenesis in *MED12* mutation-negative tumors.

Mutations in exon 2 of the *MED12* gene, the Mediator complex subunit 12, are the most common alteration in human UL (*Supplemental Fig. 2*). The Mediator is a multisubunit complex, composed of 30 distinct proteins and organized in three major modules (head, middle, and tail) and the CDK8 kinase module (39). The structure of the Mediator and accurate subunit organization are crucial elements in Mediator's ability to interact with DNA-binding transcription factors and RNA polymerase II transcription machinery. In our cohort of *MED12*-negative ULs, we observed multiple copy number aberrations in regions encompassing other Mediator complex genes including *MED8*, *MED18*, and *MED15* (Figs. 1 and 2). Such CNVs, detected by both karyotype and microarray studies, were absent in ULs positive for *MED12* mutations (Fig. 3), suggesting that loss of the Mediator subunits is another plausible mechanism for the impaired Mediator's normal function. We do not know which subunit or a combination of genomic aberrations is critical for the UL pathogenesis. *In vivo* experiments depleting the *MED1* subunit showed altered ability of the Mediator complex in

DNA binding, chromatin remodeling, and interaction with long noncoding RNAs (lncRNAs) (40). It is also possible that activity of the Mediator complex is affected owing to insufficiency or misplacement of activating lncRNAs involved in transcriptional initiation and regulation. We identified one UL sample (L48) with a deletion comprising a long intergenic non-protein coding RNA 340 (*CASC15*), however, such alterations might be below the detection resolution by microarray analyses and would remain undetected by WES studies. Since most if not all ULs harboring chromosomal abnormalities are also known to have some karyotypically normal cells, it is not surprising that some gross chromosomal alterations revealed by microarray in our samples went undetected by traditional karyotyping. This can be explained by distorted cell cycle of tumor cells and altered abilities to proliferate under the standard culturing conditions. We did not observe deletions of *MED12*, which is consistent with mechanistic studies showing that *MED12* variants act via gain of function (9). A case that shows a normal karyotype in cultured cells may be harboring cells with an abnormal karyotype that have failed to grow in culture. The same case may show a normal karyotype while displaying multiple chromosomal abnormalities by array CGH and SNP analysis performed on uncultured cells. It is known that ULs with 7q abnormalities are often mosaic with 46,XX cells and grow poorly in culture and lose the chromosomally abnormal cell line (41). Cases with *MED12* mutations have been reported to have both normal and abnormal karyotypes. Surprisingly, cells from ULs with a *MED12* mutation also tend to disappear in culture, while cells without the mutation, from the same UL, persist in culture, demonstrating the simultaneous presence of both mutated as well as nonmutated cells in the same sample (42). Addition of new array-based technology has eliminated the need to culture the cells, thus removing the culture bias. Since each technology has its limitations, judicious use of multiple techniques allows for the most accurate understanding of the genomic landscape. Indeed, our study brings new insights into the possible pathogenic mechanisms of ULs, which require further whole genome integrated analysis to dissect distinct pathways implicated in tumor initiation and progression, as well as genetic or environmental predisposing factors.

We also examined the *MED12* exon 2 mutational landscape of malignant smooth muscle tumors or LMs. In all, we examined *MED12* exon 2 variants in 153 ULMs, which is the largest cohort of ULMs examined thus far for *MED12* exon 2 variants. We determined that approximately 5% of ULMs harbor *MED12* exon 2 variants. These findings are consistent with previous studies (10,43–46) and suggest that a small subset of LMs share *MED12* exon 2 variants with ULs (*Supplemental Table 5*), but whether the molecular pathogenesis is shared between the benign and malignant counterparts, and whether other mutations need to be present, remains to be determined. Future functional studies in relevant models are required to elucidate interactions of various genomic imbalances and their relevance to pathogenesis of ULs and ULMs.

Acknowledgments: The authors thank Megan McGuire, Lori Hoffner, and Huaiyang Jiang for the technical assistance with Sanger sequencing, cytogenetics, and WES analysis and data interpretation and Drs. Dina Lev and Stephen C. Cercone for the assistance in tumor collection, classification and characterization.

REFERENCES

1. Cramer SF, Patel A. The frequency of uterine leiomyomas. *Am J Clin Pathol* 1990;94:435–8.
2. Baird DD, Dunson DB, Hill MC, Cousins D, Schectman JM. High cumulative incidence of uterine leiomyoma in black and white women: ultrasound evidence. *Am J Obstet Gynecol* 2003;188:100–7.
3. Carneiro MM. Stem cells and uterine leiomyomas: What is the evidence? *JBRA Assist Reprod* 2016;20:33–7.
4. Ono M, Bulun SE, Maruyama T. Tissue-specific stem cells in the myometrium and tumor-initiating cells in leiomyoma. *Biol Reprod* 2014;91:149.
5. Ligon AH, Morton CC. Genetics of uterine leiomyomata. *Gene Chromos Cancer* 2000;28:235–45.
6. Mäkinen N, Mehine M, Tolvanen J, Kaasinen E, Li Y, Lehtonen HJ, et al. MED12, the mediator complex subunit 12 gene, is mutated at high frequency in uterine leiomyomas. *Science* 2011a;334:252–5.
7. McGuire MM, Yatsenko A, Hoffner L, Jones M, Surti U, Rajkovic A. Whole exome sequencing in a random sample of North American women with leiomyomas identifies MED12 mutations in majority of uterine leiomyomas. *PLoS One* 2012;7:e33251.
8. Mehine M, Kaasinen E, Mäkinen N, Katainen R, Kämpäjärvi K, Pitkänen E, et al. Characterization of uterine leiomyomas by whole-genome sequencing. *N Engl J Med* 2013;369:43–53.
9. Mittal P, Shin YH, Yatsenko SA, Castro CA, Surti U, Rajkovic A. Med12 gain-of-function mutation causes leiomyomas and genomic instability. *J Clin Invest* 2015;125:3280–4.
10. Ravegnini G, Mariño-Enriquez A, Slater J, Eilers G, Wang Y, Zhu M, et al. MED12 mutations in leiomyosarcoma and extrauterine leiomyoma. *Mod Pathol* 2013;26:743–9.
11. Hu J, Surti U. Subgroups of uterine leiomyomas based on cytogenetic analysis. *Hum Pathol* 1991;22:1009–16.
12. van Beers EH, Joosse SA, Ligtenberg MJ, Fles R, Hogervorst FB, Verhoef S, et al. A multiplex PCR predictor for aCGH success of FFPE samples. *Br J Cancer* 2006;94:333–7.
13. Yatsenko SA, Bakos HA, Vitullo K, Kedrov M, Kishore A, Jennings BJ, et al. High-resolution microarray analysis unravels complex Xq28 aberrations in patients and carriers affected by X-linked blue cone monochromacy. *Clin Genet* 2016;89:82–7.
14. Mäkinen N, Heinonen HR, Moore S, Tomlinson IP, van der Spuy ZM, Aaltonen LA. MED12 exon 2 mutations are common in uterine leiomyomas from South African patients. *Oncotarget* 2011;2:966–9.
15. Wang H, Ye J, Qian H, Zhou R, Jiang J, Ye L. High-resolution melting analysis of MED12 mutations in uterine leiomyomas in Chinese patients. *Genet Test Mol Biomarkers* 2015;19:162–6.
16. Sadeghi S, Khorrami M, Amin-Beidokhti M, Abbasi M, Kamalian Z, Irani S, et al. The study of MED12 gene mutations in uterine leiomyomas from Iranian patients. *Tumour Biol* 2016;37:1567–71.
17. Kämpäjärvi K, Park MJ, Mehine M, Kim NH, Clark AD, Bützow R, et al. Mutations in Exon 1 highlight the role of MED12 in uterine leiomyomas. *Hum Mutat* 2014;35:1136–41.
18. Mas A, Cervelló I, Fernández-Álvarez A, Faus A, Díaz A, Burgués O, et al. Overexpression of the truncated form of High Mobility Group A proteins (HMGA2) in human myometrial cells induces leiomyoma-like tissue formation. *Mol Hum Reprod* 2015;21:330–8.
19. Mehine M, Kaasinen E, Heinonen HR, Mäkinen N, Kämpäjärvi K, Sarvilinna N, et al. Integrated data analysis reveals uterine leiomyoma subtypes with distinct driver pathways and biomarkers. *Proc Natl Acad Sci U S A* 2016;113:1315–20.
20. Mäkinen N, Vahteristo P, Bützow R, Sjöberg J, Aaltonen LA. Exomic landscape of MED12 mutation-negative and -positive uterine leiomyomas. *Int J Cancer* 2014;134:1008–12.
21. Santra M, Skorski T, Calabretta B, Lattime EC, Iozzo RV. De novo decorin gene expression suppresses the malignant phenotype in human colon cancer cells. *Proc Natl Acad Sci U S A* 1995;92:7016–20.
22. Järvinen TA, Prince S. Decorin: a growth factor antagonist for tumor growth inhibition. *Biomed Res Int* 2015;2015:654765.
23. Berto AG, Sampaio LO, Franco CR, Cesar RM Jr, Michelacci YM. A comparative analysis of structure and spatial distribution of decorin in human leiomyoma and normal myometrium. *Biochim Biophys Acta* 2003;1619:98–112.
24. Barker NM, Carrino DA, Caplan AI, Hurd WW, Liu JH, Tan H, et al. Proteoglycans in leiomyoma and normal myometrium: abundance, steroid hormone control, and implications for pathophysiology. *Reprod Sci* 2016;23:302–29.
25. Bidgoli SA, Khorasani H, Keihan H, Sadeghipour A, Mehdizadeh A. Role of endocrine disrupting chemicals in the occurrence of benign uterine leiomyomata: special emphasis on AhR tissue levels. *Asian Pac J Cancer Prev* 2012;13:5445–50.
26. Khorram O, Garthwaite M, Golos T. Uterine and ovarian aryl hydrocarbon receptor (AHR) and aryl hydrocarbon receptor nuclear translocator (ARNT) mRNA expression in benign and malignant gynaecological conditions. *Mol Hum Reprod* 2002;8:75–80.
27. Gong B, Hu H, Chen J, Cao S, Yu J, Xue J, et al. Caprin-1 is a novel microRNA-223 target for regulating the proliferation and invasion of human breast cancer cells. *Biomed Pharmacother* 2013;67:629–36.
28. Sabile AA, Arlt MJ, Muff R, Husmann K, Hess D, Bertz J, et al. Caprin-1, a novel Cyr61-interacting protein, promotes osteosarcoma tumor growth and lung metastasis in mice. *Biochim Biophys Acta* 2013;1832:1173–82.
29. Qiu YQ, Yang CW, Lee YZ, Yang RB, Lee CH, Hsu HY, et al. Targeting a ribonucleoprotein complex containing the caprin-1 protein and the c-Myc mRNA suppresses tumor growth in mice: an identification of a novel onco-target. *Oncotarget* 2015;6:2148–63.
30. Li L, Martinez SS, Hu W, Liu Z, Tjian R. A specific E3 ligase/deubiquitinase pair modulates TBP protein levels during muscle differentiation. *Elife* 2015;4:e08536.
31. Kurokawa M, Kim J, Geradts J, Matsuura K, Liu L, Ran X, et al. A network of substrates of the E3 ubiquitin ligases MDM2 and HUWE1 control apoptosis independently of p53. *Sci Signal* 2013;6:ra32.
32. Vaughan L, Tan CT, Chapman A, Nonaka D, Mack NA, Smith D, et al. HUWE1 ubiquitylates and degrades the RAC activator TIAM1 promoting cell-cell adhesion disassembly, migration, and invasion. *Cell Rep* 2015;10:88–102.
33. Mandai K, Rikitake Y, Shimono Y, Takai Y. Afadin/AF-6 and canoe: roles in cell adhesion and beyond. *Prog Mol Biol Transl Sci* 2013;116:433–54.
34. Kodama T, Newberg JY, Kodama M, Rangel R, Yoshihara K, Tien JC, et al. Transposon mutagenesis identifies genes and cellular processes driving epithelial-mesenchymal transition in hepatocellular carcinoma. *Proc Natl Acad Sci U S A* 2016;113:E3384–93.
35. Chen D, Kon N, Li M, Zhang W, Qin J, Gu W. ARF-BP1/Mule is a critical mediator of the ARF tumor suppressor. *Cell* 2005;121:1071–83.
36. Adhikary S, Marinoni F, Hock A, Hulleman E, Popov N, Beier R, et al. The ubiquitin ligase HectH9 regulates transcriptional activation by Myc and is essential for tumor cell proliferation. *Cell* 2005;123:409–21.
37. Hall JR, Kow E, Nevis KR, Lu CK, Luce KS, Zhong Q, et al. Cdc6 stability is regulated by the Huwe1 ubiquitin ligase after DNA damage. *Mol Biol Cell* 2007;18:3340–50.
38. Zhao X, Heng JI, Guardavaccaro D, Jiang R, Pagano M, Guillemot F, et al. The HECT-domain ubiquitin ligase Huwe1 controls neural differentiation and proliferation by destabilizing the N-Myc oncoprotein. *Nat Cell Biol* 2008;10:643–53.
39. Tsai KL, Tomomori-Sato C, Sato S, Conaway RC, Conaway JW, Asturias FJ. Subunit architecture and functional modular rearrangements of the transcriptional mediator complex. *Cell* 2014;157:1430–44.

40. Lai F, Orom UA, Cesaroni M, Beringer M, Taatjes DJ, Blobel GA, et al. Activating RNAs associate with Mediator to enhance chromatin architecture and transcription. *Nature* 2013;494:497–501.
41. Xing YP, Powell WL, Morton CC. The del(7q) subgroup in uterine leiomyomata: genetic and biologic characteristics. Further evidence for the secondary nature of cytogenetic abnormalities in the pathobiology of uterine leiomyomata. *Cancer Genet Cytogenet* 1997;98:69–74.
42. Markowski DN, Tadayon M, Bartrnitzke S, Belge G, Helmke MB, Bullerdiek J. Cell cultures in uterine leiomyomas: rapid disappearance of cells carrying MED12 mutations. *Gene Chromos Cancer* 2014;53:317–23.
43. Kämpärvi K, Mäkinen N, Kilpivaara O, Arola J, Heinonen HR, Böhm J, et al. Somatic MED12 mutations in uterine leiomyosarcoma and colorectal cancer. *Br J Cancer* 2012;107:1761–5.
44. Pérot G, Croce S, Ribeiro A, Lagarde P, Velasco V, Neuville A, et al. MED12 alterations in both human benign and malignant uterine soft tissue tumors. *PLoS One* 2012;7:e40015.
45. de Graaff MA, Cleton-Jansen AM, Szuhai K, Bovée JV. Mediator complex subunit 12 exon 2 mutation analysis in different subtypes of smooth muscle tumors confirms genetic heterogeneity. *Hum Pathol* 2013;44:1597–604.
46. Bertsch E, Qiang W, Zhang Q, Espona-Fiedler M, Druschitz S, Liu Y, et al. MED12 and HMGA2 mutations: two independent genetic events in uterine leiomyoma and leiomyosarcoma. *Mod Pathol* 2014;27:1144–53.
47. Fuentes Fajardo KV, Adams D, NISC Comparative Sequencing Program, Mason CE, Sincan M, Tiffet C, et al. Detecting false-positive signals in exome sequencing. *Hum Mutat* 2012;33:609–13.
48. Adams DR, Sincan M, Fuentes Fajardo K, Mullikin JC, Pierson TM, Toro C, et al. Analysis of DNA sequence variants detected by high-throughput sequencing. *Hum Mutat* 2012;33:599–608.

SUPPLEMENTAL DATA

WES: Data Alignment and Variant Calling

WES was performed using Illumina Hiseq 25000 providing the reads length of 100 bp. The following samples, L34/M34; L42/M42; L48/M48; L49/M49; L60/M60; L64/M64; L68/M68; L69/M69; and L70/M70, were run four per a flow cell lane, generating about 100 million reads per sample. Samples L58/M58; L59/M59 were run one per lane, producing ~400 million reads per sample. Two samples, L4/M4 and L5/M5, were subjected to in-solution exome enrichment via the SureSelect Human All Exon Kit v3 (Agilent). An average of 26 GB of data and 107,466,667 reads were generated for each sample. Data were aligned to GRCh37/hg 19 using Burrows-Wheeler Aligner's Smith-Waterman alignment algorithm, version 0.7.3a maximum exactly match (PMID: 20080505). Local realignment around indels, reads base quality recalibration, and variant calling was conducted using the

Genome Analysis Toolkit (GATK), version 2.5-2. We used both Unified Genotyper and Haplotype Caller to call variants. We also recalibrated the variants to get high-quality call.

Variants were filtered for quality, using the GATK suggested hard filter criteria. Variants were then filtered out if [1] coverage was less than 10, [2] if the alternative allele was not called in more than four reads, or [3] if the same genotype was called between leiomyoma and matched myometrium. Remaining variants were annotated using ANNOVAR (last change date: February 11, 2013). Variants were further filtered to keep the variants that were in exons or splice sites, were nonsynonymous mutations, and had an allele frequency of less than 1% in the 1000 Genomes database and/or the ESP6500 database from the National Heart, Lung, and Blood Institute. Variants were also removed if they appeared on the National Institutes of Health list of highly polymorphic (47) and frequently mutated gene lists (48).

SUPPLEMENTAL TABLE 1

Total number of copy number alterations and mutation detected in each UL sample.

Sample no.	X-HR arrays	Whole genome array	WES
L4	0	NP	0
L5	0	NP	0
L33	0	1	NP
L34	3	0	0
L42	0	0	0
L48	2	1	1
L49	1	0	2
L56	0	10	NP
L58	NP	13	3
L59	0	0	8
L63	NP	1	NP
L60	NP	1	1
L64	NP	9	1
L68	1	0	0
L69	NP	5	0
L70	NP	1	0

Note: NP = not performed.

Yatsenko. Genomic landscape of uterine leiomyomas. *Fertil Steril* 2016.

SUPPLEMENTAL TABLE 2

Abnormal G-banding findings in *MED12*-negative leiomyoma samples.

UL no.	Abnormal karyotype	Genes
1.	46,XX,del(7)(q22q32)[1]/46,XX,idem,del(14)(q22q24.3)[3]/46,XX, idem,add(1)(p13),del(14)(q22q24)[9]	Complex, multiple MED genes
2.	46,XX,rea(1),del(4)(p12),add(6)(p22),del(10)(q24)	Multiple MED genes
3.	46,XX,t(11;12)(q14.2;q13.3)	12q14 rearrangement (<i>HMGAA2</i>)
4.	46,XX,t(12;14)(q14;q23)/45,XX,idem,dic(1;22)(q42;q13)/45,XX,idem, dic(1;20)(q31;q13)	12q14 rearrangement (<i>HMGAA2</i>)
5.	46,XX,t(4;9;12)(q23;p22;q13)	12q14 rearrangement (<i>HMGAA2</i>)
6.	46,XX,del(2)(p23),add(2)(q32),del(9)(q22q32),del(13)(q13)	
7.	46,XX,del(1)(q32.1q41)	FH, multiple
8.	46,XX,del(7)(q11.2q22)	
9.	45,XX,der(1)t(1;14;16)t(1;12;14)(p31;q14;q22),dup(5)(q31q35)	12q14 rearrangement (<i>HMGAA2</i>)
10.	46,XX,-1,der(3)t(3;8;17;?)(q21;q11;q12;?);+r	Complex, multiple MED genes
11.	46,XX,-2,-13,der(22)t(2;22)(q13;q12),der(22)t(22;?)(q12;?);+mar,+r	
12.	46,XX,del(10)(q22q24)	
13.	46,XX,t(12;18)(q11;q21)	
14.	82-85,XX,+dmin	
15.	46,XX,del(1)(q32.1q42.3)	FH, multiple
16.	42,XX,t(2;18)(p23;q12)-14,-15,-19,-22	Multiple MED genes
17.	46,X,-X,r(1)(p36q44),add(2)(p13),add(4)(q21),add(8)(q22),der(9)t(9;12) (q34;q13),del(11)(q23),-12,-2,+3~4mar	Complex, multiple MED genes
18.	45,XX,del(1)(p21),-2,der(4)t(4;9;15;?)(15qter->15q15::?::4p15.2->4q22: : 9q21->9qter),-9-15,add(17)(q21),add(17)(q23),+2mar	Complex, multiple MED genes

Yatsenko. Genomic landscape of uterine leiomyomas. *Fertil Steril* 2016.

SUPPLEMENTAL TABLE 3

High-resolution X-chromosome array CGH results in *MED12* mutation-negative leiomyomas.

Sample	Chromosome	Gain/loss	Coordinates, hg19	Size, bp	Genes
L34	Xp11.22	Gain	chrX:53,631,504-53,631,825	322	<i>HUWE1</i> , exon 23
	Xq21.31	Gain	chrX:90,686,358-90,696,356	1,111	<i>PABPC5</i>
	Xq22.3	Gain	chrX:107,431,572-107,431,922	351	<i>COL4A6</i> , exon 21
L48	Xp11.23	Loss	chrX:48,890,990-48,891,667	678	<i>TFE3</i> , exons 6-8
	Xq22.1	Loss	chrX:100,872,041-100,873,269	1,229	<i>ARMCX6</i> , exons 1-3
L49	Xq28	Gain	chrX:154,391,883-154,465,363	73,481	<i>VBP1</i>
L68	Xq12	Gain	chrX:65,788,365-65,933,006	144,642	<i>EDA2R</i>

Yatsenko. Genomic landscape of uterine leiomyomas. *Fertil Steril* 2016.

SUPPLEMENTAL TABLE 4

Somatic alterations revealed by whole genome microarray analysis in *MED12* mutation negative leiomyomas.

Sample	Chromosome	Chromosome band	Gain/Loss	Coordinates, hg19	Size, bp	No. of genes	Possible target genes in the region
L33	1	q43q44	Loss	chr1:239,072,431-249,250,621	10,178,191	163	<i>FH</i>
L48	6	p22.3	Loss	chr6:21,968,899-22,182,491	213,593	2	<i>CASC15</i>
L56	1	p36.33p13.2	Loss	chr1:62,564-115,642,818	115,580,255	1721	<i>MED8, MED18, NRAS</i>
	2	p25.3p23.2	Loss	chr2:18,674-28,636,740	28,618,067	269	
	2	q35	Loss	chr2:218,674,484-218,853,391	178,908	2	<i>TNS1</i>
	7	p22.1	Loss	chr7:6,203,231-6,366,312	163,082	1	<i>CYTH3</i>
	7	p15.2	Loss	chr7:26,371,279-27,303,632	932,354	30	<i>HOXA10</i>
	7	p14.1	Loss	chr7:41,094,298-41,762,747	668,450	3	<i>INHBA</i>
	7	p14.1	Loss	chr7:42,171,041-42,428,579	257,539	1	<i>GLI3</i>
	7	q21.13q22.1	Loss	chr7:90,904,938-102,334,106	11,429,169	228	<i>CUX1, ZNHIT1</i>
	19	q11q13.33	Loss	chr19:27,732,159-49,313,242	20,646,185	867	<i>MED29</i>
	20	p13q13.33	Gain	chr20:6,477,557-24,649,936	18,172,380	175	
L58	1	p36.33p35.2	Loss	chr1:58,411-32,073,316	32,014,906	646	<i>MED18</i>
	2	p25.3p21	Loss	chr2:17,019-44,577,643	44,560,625	408	
	2	p25.3p16.1	Loss	chr2:17,019-61,011,618	60,994,600	519	
	6	p25.3p21.1	Loss	chr6:206,749-44,146,874	43,940,126	914	<i>MED20, CASC15</i>
	6	p12.3q16.1	Loss	chr6:47,214,638-97,466,997	50,252,360	366	
	6	q16.1q27	Loss	chr6:98,762,425-170,890,108	72,127,684	648	<i>CCNC, CDK19, MED23</i>
	8	p23.3p12	Loss	chr8:191,530-34,250,792	34,059,263	440	
	13	q12.11	Loss	chr13:21,552,490-22,051,938	499,449	15	
	13	q12.12	Loss	chr13:23,922,218-24,827,740	905,523	14	
	13	q12.13q21.2	Loss	chr13:26,319,821-60,225,494	33,905,674	395	<i>CDK8, MED4</i>
	13	q34	Loss	chr13:113,814,783-115,092,648	1,277,866	30	
	17	p13.2p13.1	Loss	chr17:3,546,091-10,127,707	6,581,617	216	<i>MED11, MED31</i>
	22	q11.1q12.3	Loss	chr22:16,915,658-35,730,045	18,814,388	508	<i>MED15</i>
L60	6	q22.31q23.3	Loss	chr6:125,609,217-137,926,848	12,317,632	138	<i>MED23</i>
L63	3	p26.3q29	Loss	chr3:62,199-197,861,598	197,799,400	2,048	<i>MED12L</i>
L64	1	q32.2q42.2	Loss	chr1:210,369,136-234,105,211	23,736,076	295	
	9	q31.1	Loss	chr9:106,045,690-108,152,430	2,106,740	23	
	11	q13.4q23.3	Loss	chr11:72,111,539-114,739,736	42,628,197	472	<i>MED17</i>
	11	q23.3	Loss	chr11:117,010,323-120,360,191	3,349,868	85	
	11	q24.1	Loss	chr11:121,265,513-122,640,790	1,375,277	8	
	12	q14.1	Loss	chr12:66,364,509-66,622,071	257,563	7	3'-UTR <i>HMGA2</i>
	15	q21.3	Loss	chr15:57,307,488-57,633,211	325,723	5	
	15	q24.3	Loss	chr15:76,616,542-76,853,202	236,660	3	
	15	q25.1	Loss	chr15:79,321,450-80,730,546	1,409,096	22	

Yatsenko. Genomic landscape of uterine leiomyomas. *Fertil Steril* 2016.

SUPPLEMENTAL TABLE 4

Continued.

Sample	Chromosome	Chromosome band	Gain/Loss	Coordinates, hg19	Size, bp	No. of genes	Possible target genes in the region
L69	1	p36.33p32.1	Loss	chr1:82,154-61,264,038	61,181,885	1,149	<i>MED8, MED18</i>
	1	p32.1q32.3	Gain	chr1:61,265,635-212,351,181	151,085,547	1,896	
	1	q32.3	Loss	chr1:212,370,745-213,168,459	797,715	20	
	1	q32.3q41	Gain	chr1:213,181,916-215,124,414	1,942,499	14	
	1	q41q44	Loss	chr1:215,126,030-249,212,429	34,086,400	463	<i>FH</i>
L70	3	p26.3q29	Loss	chr3:62,199-197,861,598	197,799,400	2,048	<i>MED12L</i>

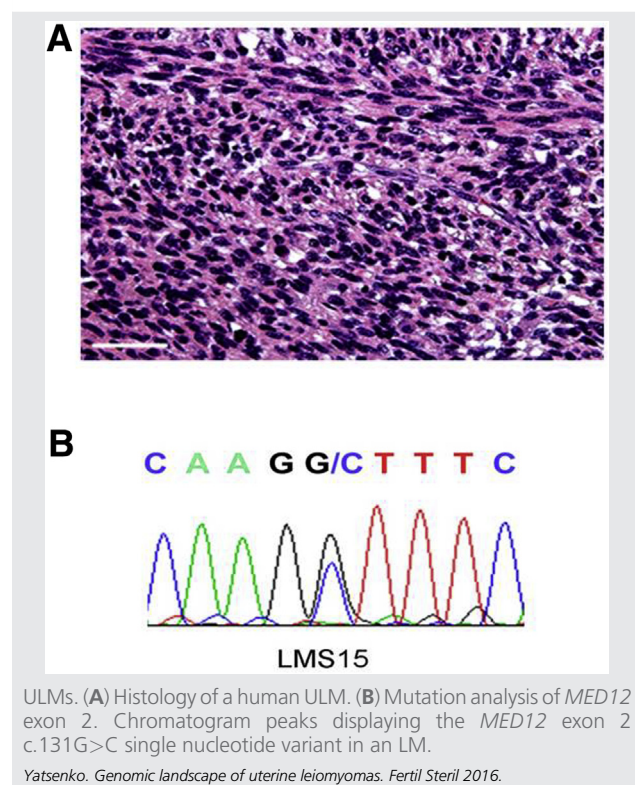
Yatsenko. Genomic landscape of uterine leiomyomas. *Fertil Steril* 2016.

SUPPLEMENTAL TABLE 5

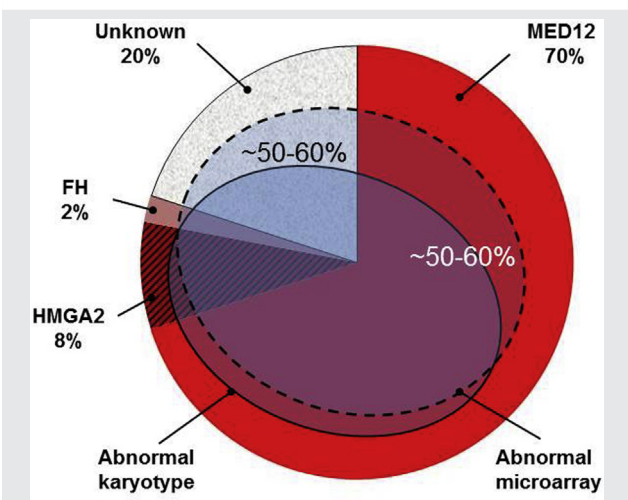
Meta-analysis of <i>MED12</i> exon 2 somatic mutations in ULMs.		
Study (reference)	Population	<i>MED12</i> exon 2 mutations (%)
Kämpäjärvi et al., 2012 (43)	Finnish	3/41 (7)
Pérot et al., 2012 (44)	French	2/10 (20)
de Graaff et al., 2013 (45)	Dutch	1/7 (14.2)
Ravegnini et al., 2013 (10)	North American	3/27 (11.1)
Bertsch et al., 2014 (46)	American	3/32 (9.4)
This study	North American	7/153 (4.6)
Total		19/238 (8)

Yatsenko. Genomic landscape of uterine leiomyomas. *Fertil Steril* 2016.

SUPPLEMENTAL FIGURE 1



SUPPLEMENTAL FIGURE 2



Pie chart showing the distribution of somatic clinically relevant genomic alterations identified to date in human ULs. Gross numerical and structural chromosomal abnormalities are detected by karyotype in ~50%–60% of the samples. In our study, up to ~65% of karyotypically normal samples were found to have large or submicroscopic genomic alterations detected by microarray.

Yatsenko. Genomic landscape of uterine leiomyomas. *Fertil Steril* 2016.